

# **Out-of-network events can be of great importance for improving results of local earthquake tomography**

5

10

Ivan Koulakov,

Institute of Petroleum Geology and Geophysics, SB RAS,  
Prospekt Akademika Koptuga, 3, Novosibirsk, 630090, Russia

15

e-mail: KoulakovIY@ipgg.nsc.ru

Phone: +7 383 3309201

20

submitted to BSSA

second revision

25

30

Novosibirsk, March 2008

## Abstract

35

In most local earthquake tomography (LET) studies the data are selected according to the azimuthal-gap (GAP) criterion which means rejecting all the sources outside the station network perimeter. In this paper we show that in some cases this criterion is inappropriate and can be a reason for significant decimation of the relevant data, in turn leading to lower quality inversion results. This study presents several qualitative and quantitative arguments why the GAP criterion is not adequate. The fact of great importance of out-of-network events for improving the results of tomographic inversion is supported by synthetic testing using realistic distribution of events in the area of Central Java and station locations according to the MERAMEX Project. I consider three datasets with different criteria of event selection: (1) with  $GAP < 180^\circ$ ; (2) with  $GAP < 280^\circ$ ; and (3) dataset with all events within a radius of  $5^\circ$ . The synthetic modeling reproduces the real situation when neither coordinates of sources nor starting 1D models are initially known. The reconstruction results show that the best resolution is obtained for the model (3) with all data available, while the worst solution is observed in the case (1). This study demonstrates that the commonly used GAP criterion which rejects the out-of-network events is injurious for LET tomography. In future experiments and when reconsidering the old datasets, we encourage using the data from all events, though at large distances from networks (as least, up to 400-500 km), to improve the results of tomographic inversion.

55

## 60 Introduction

Here I consider a problem of data selection when performing local earthquake tomography (LET). There is a presumption widely held in the tomographic community, that sources located outside the perimeter of the station network are useless for performing tomographic inversion. In most LET algorithms (see examples in [Thurber et al., 1995](#); [Husen et al., 2000, 2003, 2004](#); [Husen and Smith, 2004](#); [Vlahovic and Powel, 2001](#); [Barberi et al., 2004](#); [Reyners et al., 2006](#); [Daly et al., 2008](#); [Chiarabba and Amato, 2003](#); [Paul et al., 2001](#); [Dias et al.,](#)

2007; and many other), all sources located outside the network are rejected *a priori*. To make this selection, a GAP criterion, the maximum empty azimuthal angle, is used. In these studies events having a GAP of more than  $180^\circ$  are rejected. Even if the GAP criterion is not mentioned directly in some studies (e.g. Kato et al., 2007; Eberhart-Phillips and Bannister, 2002), the presented figures show that only events located inside the network perimeter are used in majority of the LET studies. This criterion is grounded on an assumption that the accuracy of source locations inside the network is better than those outside. In most studies, using the GAP criterion significantly shrinks the data set. Nevertheless, the authors of such works believe that this criterion increases the reliability of the results. At the same time, I could not find in the literature any appropriate argumentation which confirmed the statement that rejecting the out-of-network data according to the GAP criterion really improves the results of tomographic inversion. Taking into account the costs of a network deployment and maintaining the stations during an experiment, throwing out a considerable part of the data just because of this ungrounded criterion seems to be unacceptable. Therefore it is a matter of great importance to confirm or disprove the efficiency of the GAP criterion based on quantitative estimates. The main purpose of this paper is to explore the effect of adding/rejecting the out-of-network sources upon the results of tomographic inversion using synthetic modeling.

## 85 Qualitative arguments against using the GAP criterion in LET

The statement that the accuracy of out-of-network source locations is lower, and the error increases with distance from the network, seems to be intuitively reasonable and it is correct in most cases. However, there are some obvious exceptions. For example, an event located slightly outside the network and having 100 clear picks will probably be much better determined than another event located inside the network and having only ten noisy picks. However, in most LET studies which use the GAP criterion, the former event is rejected and the latter is used in processing.

Second, introducing the GAP criterion in most algorithms presumes computing the angles in horizontal projection. However, it is clear that the accuracy of source location depends on the GAP value in three dimensions. When sources are located below a certain depth for surface station arrays of finite extent, the 3D GAP is always greater than  $180^\circ$ , that is no down going rays are observed at the source. The deeper a source is, the greater will be its 3D GAP and the lower the accuracy of the source location. In some current LET schemes, using the 2D GAP criterion creates the dubious situation illustrated in Figure 1. A shallow source located just a few kilometers outside the network is rejected (circles in clusters 1 and 2) while an earthquake

several hundreds of kilometers deep (crosses in cluster 3) is taken into consideration. It is likely that the former events are better located than the deep events.

However, even if one accept, for argument's sake, that location accuracy outside the network is low, it does not follow *a priori* that these events are useless for deriving the velocity structure. For example, in tomographic schemes based on using the teleseismic rays from remote events (see examples in [Aki et al., 1977](#); [Evans and Achauer, \(1993\)](#); [Lippitsch et al., 2003](#); [Sandoval et al., 2004](#); and many others), which represent an extreme case of large GAP, the source parameters are taken from international catalogues and errors in their location are often rather large. Nevertheless this constraint does not cause practical trouble when performing tomographic inversions. In LET algorithms where the GAPs for the events outside the network are much more reasonable, the problem of source uncertainty is less dramatic. I claim that adding sources located outside the network perimeter does not cause a problem in LET inversions and in most cases improves the resolution of the resulting velocity model. In this paper I present examples of synthetic modeling which disprove the assertion that the GAP criterion is appropriate in LET schemes.

## Synthetic modeling

The synthetic modeling has been performed using our LOTOS-07 algorithm for LET inversion (e.g., [Koulakov et al., 2007](#), [Koulakov, 2009](#) and on our Web site, see the Data and Resources section). Set up of the synthetic model and data processing represent as close as possible the realistic situation. The distribution of stations ([Figure 2 A](#)) corresponds to a real experiment in Central Java performed in 2005 in the framework of the MARAMEX Project ([Koulakov et al., 2007](#)). Part of the events are taken from the real catalogue of seismicity recorded during the experiment. Unfortunately when the processing of the initial data was performed, the operators who picked the phases were under the pressure of the GAP stereotype, and they did not pay much attention to collecting out-of-network events. Only few of them were detected in the final stage of picking. Ideally, these data should be reprocessed, but unfortunately we do not have either human or financial resources to repeat this routine work. In the modeling presented in this study, the MARAMEX dataset was supplemented with 500 ISC events ([ISC, 2001](#)) located within a radius of  $5^\circ$  with respect to the center of the network ( $110^\circ\text{E}$  and  $8^\circ\text{S}$ ). For the MARAMEX events we used the same source-receiver (S-R) pairs as in the observed dataset. For the ISC events the S-R pairs were generated artificially. For such events the number of P picks varied randomly from 0 to 50. The stations for each S-R pair were selected randomly.

For 20% - 60% of the randomly selected S-R pairs having P picks we created S picks. After  
135 generating the dataset, the events with less than 20 picks were removed from consideration.

In this study we consider three different datasets. In the first dataset we use only events  
having the  $GAP < 180^\circ$ . A total of 130 events within the area M1 in [Figure 2](#) (including 27 ISC  
events) with 4879 P and 2668 S picks were selected. In the second dataset, the allowed GAP was  
increased up to  $280^\circ$  (area M2 in [Figure 2](#)). In this case the number of events was 343 (including  
140 109 ISC events) with a corresponding 13060 P picks and 6649 S picks. In the third dataset we  
used all the events within a radius of  $5^\circ$  with respect to the center of the network (a total 838  
events including 424 ISC events, 31954 P picks and 15797 S picks). The distribution of events  
for the latter case is presented in [Figure 2](#).

The average summary number of P and S picks per event is similar in all cases (58, 57  
145 and 57 for Models 1, 2 and 3, respectively). Adequacy of the modeling setup can be grounded by  
simple estimates. In the area of about  $200 \times 300$  km size corresponding to Model 1 ( $GAP > 180^\circ$ )  
we have 130 events. The area for event selection in Model 3 is of 500 km radius, and its space is  
about 20 times larger than in the case of Model 1. Statistically, in Model 3 we can expect 20  
times more events of the same class than in Model 1 ( $\sim 2600$  events). In fact, for the specific case  
150 of Central Java experiment, the number of out-of-network events can be even larger, because the  
network is deployed in the area of relative seismic gap which is clearly observed in the ISC data.  
In the modeling we use  $\sim 700$  out-of-network events (total 838 events minus 130 events located  
inside the network). This almost four times decrease of data amount with respect to the  
statistically possible value represents the selection of events with sufficiently large magnitudes.  
155 Such out-of-network events are recorded by the similar average number of stations as the weaker  
local events located inside the network area.

A synthetic model is defined as a 3D checkerboard pattern ( $30 \times 30 \times 25$  km in size along  
the X, Y and Z directions, respectively). Anomalies of  $\pm 2\%$  amplitude are given with respect to  
the “true” 1D reference velocity distribution,  $V_{true}$  (bold black lines in Plots D in [Figures 3 to 5](#)).  
160 For sources located far outside the network, a large part of the ray paths travels outside the  
resolved area which roughly coincides with the network location. If such rays pass through  
outside velocity anomalies, they accumulate additional residuals and may bias the computed  
structure in the resolved area. In order to investigate this effect upon the velocity structure  
beneath the network, we defined the periodical checkerboard structure far outside the resolved  
165 area (in a square of  $1600 \times 1600$  km size). In the vertical direction the checkerboard is defined  
down to 150 km depth. In [Figures 3 to 5](#) the configuration of the checkerboard in vertical and  
horizontal sections is indicated with grid lines.

Synthetic travel times are computed by 3D ray tracing in the checkerboard model using our own version of the bending algorithm (Koulakov, 2009). I add the random noise with realistic RMS (0.1 s for P and 0.15 s for S data) and distribution histogram. Furthermore, the origin times of each event are perturbed with a random bias. After computing these synthetic data, I “forget” the coordinates and origin times of sources and everything about the velocity model. I then have only the coordinates of stations and randomly perturbed arrival times of P and S rays. I use a starting 1D model,  $V_{start}$  (dotted line in Plot G in Figures 3 to 5), which is presumably different from “true” values of  $V_{true}$ . Initial source coordinates are the same for all sources - the center of the network at the depth of 10 km. Sources located in the starting model and mislocation errors with respect to “true” values are shown in Figure 2 B. It can be seen that sources in the northern clusters which are located at ~600 km depth are strongly biased, that is probably related to “wrong”  $V_p/V_s$  ratio in the starting model (1.74) with respect to the “true” one (1.7).

Processing begins with the preliminary location of the sources and finding an optimal 1D model,  $V_{res}$ . The algorithm for the preliminary location of sources is based on a 1D velocity model and uses tabulated travel times. This allows performing grid searching for the hypocenter coordinates which is rather fast and stable, even when a true event is located far from the initial point of search (e.g., at distances of 400-500 km). 1D velocity optimization is performed iteratively in parallel with the grid search location of sources. The resulting distributions of the 1D P and S velocities for three considered models are shown with grey lines in Plots D in Figures 3 to 5. In all cases the retrieved velocity distribution fit the true model (black bold lines) rather well. However, for Model 3 which contains many long ray paths from the out-of-network events the optimized velocity seems to be higher than the true one. This can be explained by the fact of dominating negative residuals in the synthetic dataset caused by preferential traveling of the bending rays through positive velocity blocks.

The derived 1D distribution is used as a starting velocity model for an iterative tomographic inversion and further source relocations based on the LOTOS-07 code (Koulakov, 2009). It is important that the velocity model is computed in several parameterization grids with different predefined orientations (e.g., 0, 22, 45 and 67 degrees) and then averaged into one model. The parameterization nodes are installed according to the ray distributions. The minimal node spacing is 5 km and it is much smaller than the size of the synthetic patterns (30 km). In this case the solution is practically independent of the grid configurations and the parameterization can be called quasi-continuous. For Model 3 the numbers of parameters were ~23000 for the P model and ~21000 for the S model.

The resulting locations of events after five iterations of simultaneous inversion for velocity distribution and source parameters are shown in [Figure 2C](#). It can be seen that the 3D inversion leads to a considerable decrease of mislocation of the events. However, for events  
205 located far outside the network the error remains important. For some events it reaches 20-40 km. Nevertheless, as will be shown later, adding such events, although located with considerable error, does not prevent, but helps to improve the quality of tomographic inversion.

The results of P velocity reconstructions for the three considered models are presented in [Figures 3 to 5](#) in three horizontal and two vertical sections. The horizontal sections at depths of  
210 15, 35 and 60 km correspond to three upper layers of the different checkerboard polarities. The results for S velocity are practically identical and are not shown here. Model 1 ([Figure 3](#)), for which only events with  $GAP < 180^\circ$  were selected, provides rather poor reconstruction quality, especially in the lower section. The satisfactory reconstruction quality is only observed for the uppermost layer (15 km depth). In the second layer, only qualitative correspondence with the  
215 checkerboard structure is observed in the central part of the study area. For the third layer the reconstructed patterns seem to be chaotic. In the vertical sections the anomalies are strongly smeared diagonally. For Model 2 ([Figure 4](#)) with GAP limitation of  $280^\circ$ , the reconstruction quality is much higher. The good resolution area is larger in both horizontal and vertical sections. The uppermost two layers of the checkerboard are reconstructed robustly and in the third layer  
220 the general periodicity of anomalies is visible. However the best results are obtained for the case when all events within the radius of  $5^\circ$  are used (Model 3, [Figure 5](#)). Indeed, the checkerboard structure is robustly reconstructed in the three uppermost layers of the checkerboard. The higher quality of reconstruction in Model 3 is related to two advantageous factors of using out-of-  
225 network events: a significant increase in the amount of data and much better spatial coverage of the ray paths. Their positive contribution appears to be quite important and it completely compensates for any negative effect related to the poorer locations of out-of-network events.

Similar tests were performed for different realistic and artificial observation schemes. In particular together with my colleagues we have found the positive effect of using the out-of-  
230 network events for real networks in the area of North Anatolian fault and Toba caldera (Indonesia). However due to limited space of this short note paper we cannot present these results here.

## Conclusions

The results of three tests presented in this paper show that rejecting the sources outside  
235 the network is contraindicated or at least inadequate in LET modeling. It was shown here that for

the considered observation schemes increasing the area for the event selection improves the quality of the tomographic inversion. The same results have been obtained for several other realistic and artificial experiment configurations. I did not check larger than 5° areas for the source selection, but I suppose that adding events located at larger distances may cause further  
240 improvement of the results. It will probably lead to increase of variability of incidence angles and azimuths of rays in the target volume that is obviously favorable for tomographic inversion. In particular, I suppose that it would be very fruitful to combine local and teleseismic data. For example, in some subduction zones, deep seismic clusters in the slab are focused in narrow zones. The rays from these clusters are quasi parallel and often cause strong smearing of the  
245 resulting anomalies. If these rays are combined with teleseismic rays coming from other directions it would obviously improve the spatial resolution and would increase depth penetration of tomographic models.

At the same time I admit that I cannot consider all the variety of possible source/receiver configurations which could exist in LET schemes. Thus, I do not pretend that the statement about  
250 improving the results when out-of-network sources are used is universal in all situations. For example, I expect that adding out-of-network events which are clustered in one localized area would possibly not provide improvement of the results and might cause smearing of the resulting anomalies. On the other hand, it should be mentioned that similar effect of smearing caused by clustering may equally appear for events located inside the network, so it is not a specific  
255 problem of using out-of-network events.

The possibility of the existence of opposite cases means that the data selection criteria should be checked individually for each source/receiver configuration. The most clear and effective way is to perform synthetic modeling, such as a checkerboard test, as was done in this study, for various datasets. In my opinion, it is impossible to propose a universal scheme for data  
260 selection which would be suitable for any possible experiment setup.

In any case, the rays from events at any distances if they travel through the target area accumulate some information about the deep structure. The purpose of tomography is to decrypt it. Most of LET algorithms are not working *a-priori* with data from out-of-network events, and their users usually adapt the datasets to the existing codes and reject a lot of relevant information.  
265 It seems to me that it would be much more constructive to adapt the algorithms to the existing data and to use as much as possible of available information including events from all ranges of epicentral distances.

The strong positive effect of adding out-of-network events demonstrated in this study shows that the strategy of LET experiment performed in the commonly accepted practice should  
270 be revised. It is clear now that executing costly work on performing experiments and then



rejecting most of relevant information just because of the GAP stereotype is very inefficient. This causes strong limiting of the resolution and decreasing the scientific importance of the results. In my opinion, all the published results on local earthquake tomography which used only events with  $GAP < 180^\circ$  can be significantly improved if the authors revise their datasets and use a broader distribution of sources.

## Acknowledgements

This paper was inspired by criticism of several anonymous reviewers who rejected my previous papers just because of using a more liberal than  $GAP < 180^\circ$  selection criteria. Heated discussions with Edi Kissling were very important in constructing the argumentation scheme of this paper. I am very grateful to Andrew J. Michael for constructive suggestions on preparing this study. I thank the anonymous Associate Editor for important comments and help in editing the text of the manuscript. This study is supported by Russian Foundation for Basic Researches (08-05-00276-a), Heimboltz Society and RFBR joint research project 09-05-91321-SIG\_a, multidisciplinary projects SB RAS 44, 21 and SB-UrO-DVO RAS 96, and project ONZ RAS 7.4.

## Data and Resources

In the article we present synthetic data based on real configuration of sources and receivers corresponding to a real experiment in Central Java (Koulakov et al., 2007). A part of the events used in modeling is taken from the ISC catalogue (ISC, 2001).

The *LOTOS* code for tomographic inversion, which is used in this study, is freely available online at [www.ivan-art.com/science/LOTOS\\_09](http://www.ivan-art.com/science/LOTOS_09) (last accessed March 2009). This Internet site provides executable version of the code, its detailed description, manuals, examples of observed and synthetic datasets, and other necessary information.

The three synthetic datasets presented in this paper are available online in file: [www.ivan-art.com/science/LOTOS\\_09/data\\_for\\_lotos\\_9.zip](http://www.ivan-art.com/science/LOTOS_09/data_for_lotos_9.zip) in folders “GAP\_\_180”, “GAP\_\_280” and “GAP\_\_360”. All the pictures presented in this paper can be easily reproduced by any person by running the executable version of the LOTOS-09 code for each of these datasets.

## Figure captions

Figure 1. Sketch showing inadequacy of the GAP criterion. Crosses and circles indicate events in  
305 three clusters in a vertical profile; triangles on surface indicate station projections. It is possible  
that events in clusters 1 and 2 (circles) are better located than crosses in the deep cluster 3. At the  
same time, the GAP criterion selects only events in cluster 3 as indicated by crosses.

Figure 2. Stations and relocated sources used for modeling. A.) Stations used for modeling  
310 indicated by crosses. B.-C.) Locations of events in the starting 1D velocity model (Plot B) and  
after final iteration of 3D tomographic inversion (Plot C) are depicted with grey dots. Bars show  
errors with respect to “true” locations. Areas marked with M1 and M2 indicate the areas of event  
selection for the cases of  $GAP < 180^\circ$  and  $GAP < 280^\circ$ , respectively.

315 Figure 3. Inversion results using the sources selected according to  $GAP < 180^\circ$ . A, B and C:  
resulting P velocity anomalies in horizontal sections (contour lines are shown at levels of -2%, 0  
and 2%). Grey grid lines indicate the locations of the checkerboard anomalies in the synthetic  
model. D: result of the 1D model optimization. Black line is the true model; dotted black line is  
the starting model; bold grey line is the retrieved model. E and F: resulting velocity anomalies of  
320 P velocities in two vertical sections (positions of the sections are indicated in A-C). Grey dots are  
relocated sources at a distances of up to 200 km from the profiles; bars show errors with respect  
to true coordinates.

Figure 4. Inversion results using the sources selected according to  $GAP < 280^\circ$ . Meaning of plots  
325 and symbols are the same as in Figure 3.

Figure 5. Inversion results using all sources within the area of  $5^\circ$  with respect to the center of the  
network. Meaning of plots and symbols are the same as in Figure 3.

## References:

- 330 Aki, K., Christofferson, A. & Husebye, E.S., 1977, Determination of the three dimensional structure of the lithosphere, *J. Geophys. Res.*, v.82., P. 277-296.
- Barberi, G., M.T. Cosentino, A. Gervasi, I. Guerra, G. Neri and B. Orecchio, 2004. Crustal seismic tomography in the Calabrian Arc region, south Italy, *Phys. Earth Planet. Inter.*, 335 147, 297-314.
- Chiarabba, C., and A. Amato, 2003. Vp and Vp/Vs images in the Mw 6.0 Colfiorito fault region (central Italy): A contribution to the understanding of seismotectonic and seismogenic processes, *J. Geophys. Res.*, 2003, v.108(B5), 2248, doi:10.1029/2001JB001665.
- Daly E., D. Keir, C. J. Ebinger, G. W. Stuart, I. D. Bastow, and A. Ayele, 2008. Crustal 340 tomographic imaging of a transitional continental rift:the Ethiopian rift, *Geophys. J. Int.* 172, 1033–1048.
- Dias N.A., L. Matias, N. Lourenço, J. Madeira, F. Carrilho, and J.L. Gaspar, (2007), Crustal seismic velocity structure near Faial and Pico Islands (AZORES), from local earthquake tomography, *Tectonophysics*, 445, 301–317
- 345 Eberhart-Phillips, D., and S. Bannister, 2002, Three-dimensional crustal structure in the Southern Alps region of New Zealand from inversion of local earthquake and active source data, *J. Geophys. Res.*, v.107(B10), 2262, doi:10.1029/2001JB000567.
- Evans, J. & Achauer, U. , 1993, Teleseismic velocity tomography using the ACH method: theory and application to continental scale studies, In: Iyer, H., Hirahara, K. (Eds.). *Seismic tomography: Theory and Practice*, Chapman & Hall, London, pp. 319-360.
- 350 Husen S., E. Kissling, and E.R. Flueh, 2000, Local earthquake tomography of shallow subduction in north Chile: A combined onshore and offshore study, *J. Geophys. Res.*, 105, 28,183.
- Husen S., R. Quintero, E. Kissling, and B. Hacker, 2003. Subduction-zone structure and 355 magmatic processes beneath Costa Rica constrained by local earthquake tomography and petrological modeling, *Geophys. J. Int.*, v.155, p.11-32.
- Husen S. and R.B. Smith, 2004, Probabilistic earthquake relocation in three-dimensional velocity models for the Yellowstone National Park region, Wyoming, *Bull. Seism. Soc. Am.*, v.94, p.880-896.
- 360 Husen S., R.B. Smith, G.P. Waite, 2004. Evidence for gas and magmatic sources beneath the Yellowstone volcanic field from seismic tomographic imaging, *J. Volcanol. Geotherm. Res.*, v.131, p.397-410.
- International Seismological Centre, 2001. Bulletin Disks 1-9 [CD-ROM], Internatl. Seis. Cent.,

Thatcham, United Kingdom.

- 365 Kato, A., T. Iidaka, E. Kurashimo, S. Nakagawa, N. Hirata, and T. Iwasaki, 2007, Delineation of probable asperities on the Atotsugawa fault, central Japan, using a dense temporary seismic network, *Geophys. Res. Lett.*, 34, L09318, doi:10.1029/2007GL029604.
- Koulakov I., M. Bohm, G. Asch, B.-G. Lühr, A. Manzanares, K.S. Brotopuspito, Pak Fauzi, M. A. Purbawinata, N.T. Puspito, A. Ratdomopurbo, H.Kopp, W. Rabbel, E. Shevkunova, 370 2007, P and S velocity structure of the crust and the upper mantle beneath central Java from local tomography inversion, *J. Geophys. Res.*, 112, B08310, doi:10.1029/2006JB004712.
- Koulakov I., 2009, LOTOS code for local earthquake tomographic inversion. Benchmarks for testing tomographic algorithms, *Bulletin of the Seismological Society of America*, Vol. 99, 375 No. 1, pp. doi: 10.1785/0120080013
- Lippitsch, R., Kissling, E. & Ansorge, J., 2003, Upper-mantle structure beneath the Alpine orogen from high-resolution teleseismic tomography, *J. Geophys. Res.*, v.108(B8), p.2376–2390.
- Paul, A., M. Cattaneo, F. Thouvenot, D. Spallarossa, N. Bethoux and J. Frechet, 2001. A three- 380 dimensional crustal velocity model of the south-western Alps from local earthquake tomography, *J. Geophys. Res.*, v.106 (B9), p.19367-19389.
- Reyners, M., D. Eberhart-Phillips, G. Stuart, & Y. Nishimura, 2006. Imaging subduction from the trench to 300 km depth beneath the central North Island, New Zealand, with  $V_p$  and  $V_p/V_s$ : *J. Geophys. Res.*, 87(B5), 4073–4088.
- 385 Sandoval, S., Kissling, E., Ansorge, J., and the SVEKALAPKO STWG, 2004, High-resolution body wave tomography beneath the SVEKALAPKO array: II. Anomalous upper mantle structure beneath the central Baltic Shield, *Geophys. J. Int.*, v.157, p.200-214.
- Thurber, C. H., S. R. Atre, and D. Eberhart-Phillips, 1995, Three-Dimensional  $V_p$  and  $V_p/V_s$  Structure at Loma Prieta, California, from Local Earthquake Tomography, *Geophys. Res. 390 Lett.*, 22(22), 3079–3082.
- Vlahovic, G., and C. A. Powell, 2001. Three-dimensional S-wave velocity structure and  $V_p/V_s$  ratios in the New Madrid seismic zone, *Journal of Geophysical Research*, V. 106, no B7, 13,501-13,514.

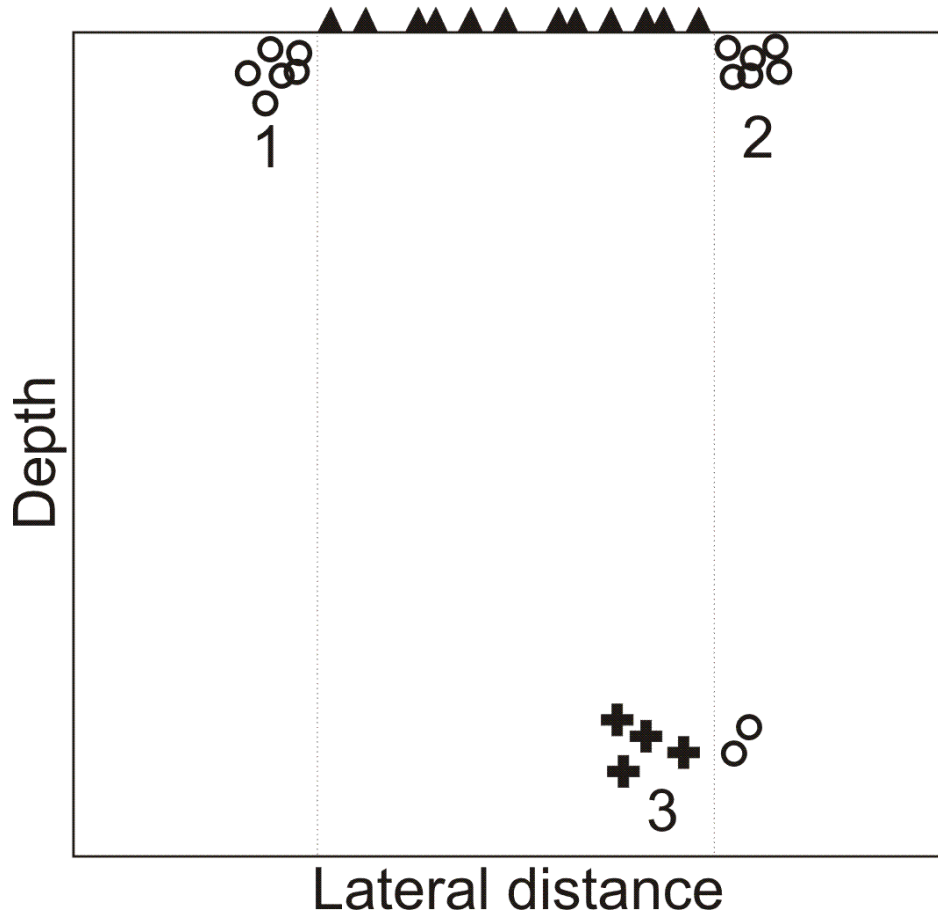
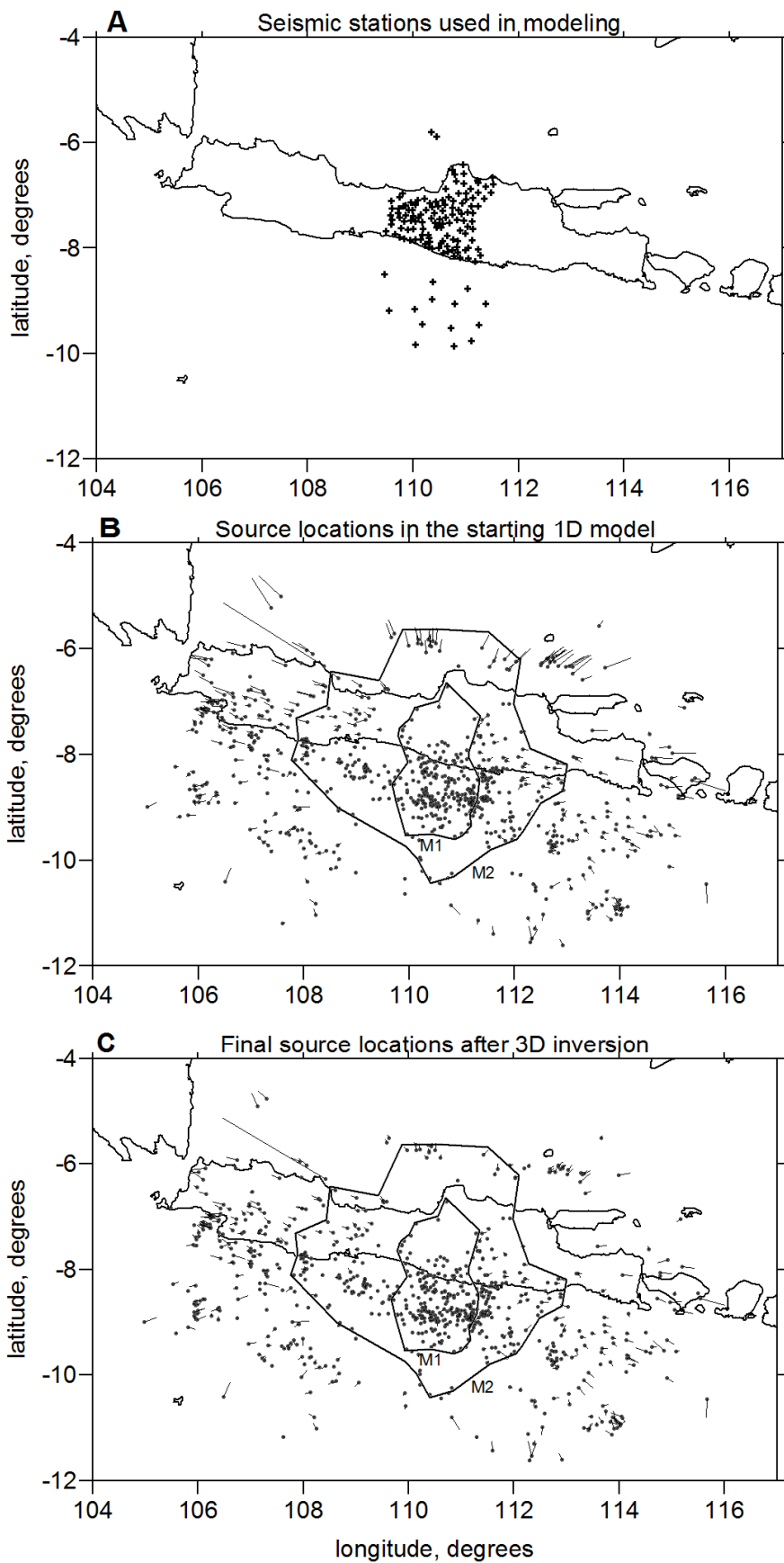


Figure 1. Sketch showing inadequacy of the GAP criterion. Crosses and circles indicate events in three clusters in a vertical profile; triangles on surface indicate station projections. It is possible that events in clusters 1 and 2 (circles) are better located than crosses in the deep cluster 3. At the same time, the GAP criterion selects only events in cluster 3 as indicated by crosses.



405 Figure 2. Stations and relocated sources used for modeling. A: Stations used for modeling indicated by crosses. B, C: Locations of events in the starting 1D velocity model (Plot B) and after final iteration of 3D tomographic inversion (Plot C) are depicted with grey dots. Bars show errors with respect to “true” locations. Areas marked with M1 and M2 indicate the areas of event selection for the cases of  $GAP < 180^\circ$  and  $GAP < 280^\circ$ , respectively.

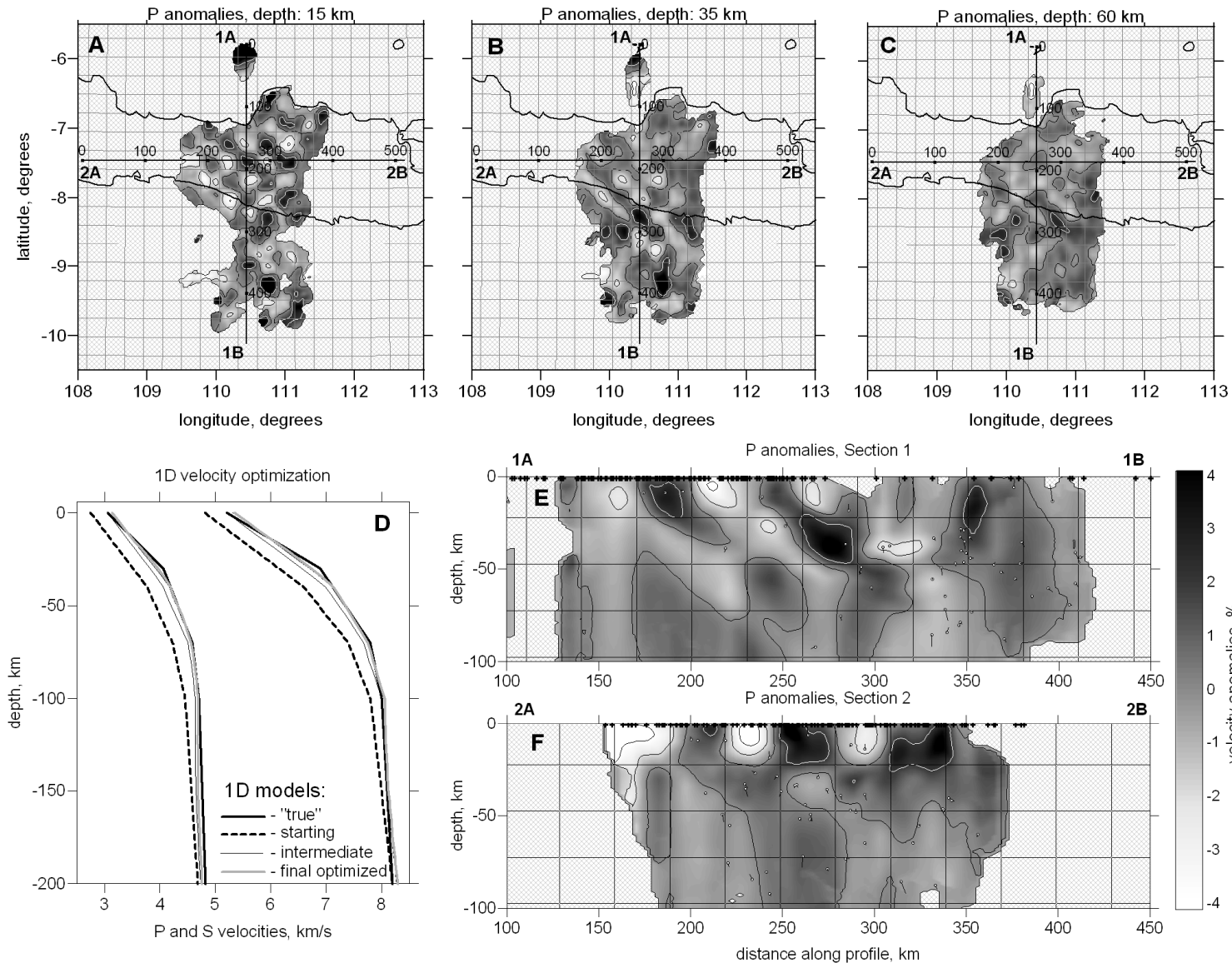


Figure 3. Inversion results using the sources selected according to  $GAP < 180^\circ$ . A, B and C: resulting P velocity anomalies in horizontal sections (contour lines are shown at levels of -2%, 0 and 2%). Grey grid lines indicate the locations of the checkerboard anomalies in the synthetic model. D: result of the 1D model optimization. Black line is the true model; dotted black line is the starting model; bold grey line is the retrieved model. E and F: resulting velocity anomalies of P velocities in two vertical sections (positions of the sections are indicated in A-C). Grey dots are relocated sources at distances of up to 200 km from the profiles; bars show errors with respect to true coordinates. (Color version: Electronic Supplementary 1)

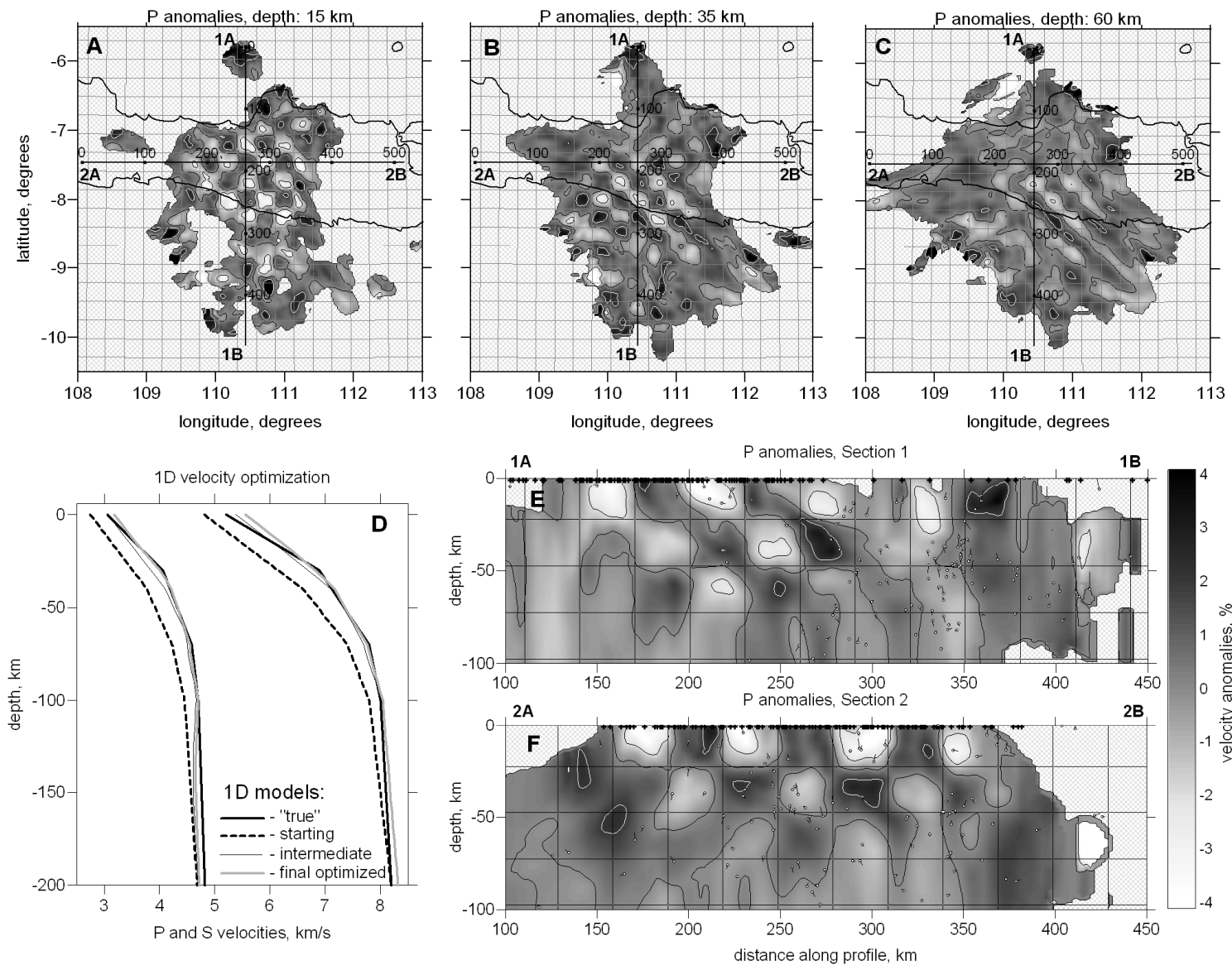


Figure 4. Inversion results using the sources selected according to  $GAP < 280^\circ$ . Meaning of plots and symbols are the same as in Figure 3. (Color version: Electronic Supplementary 2)



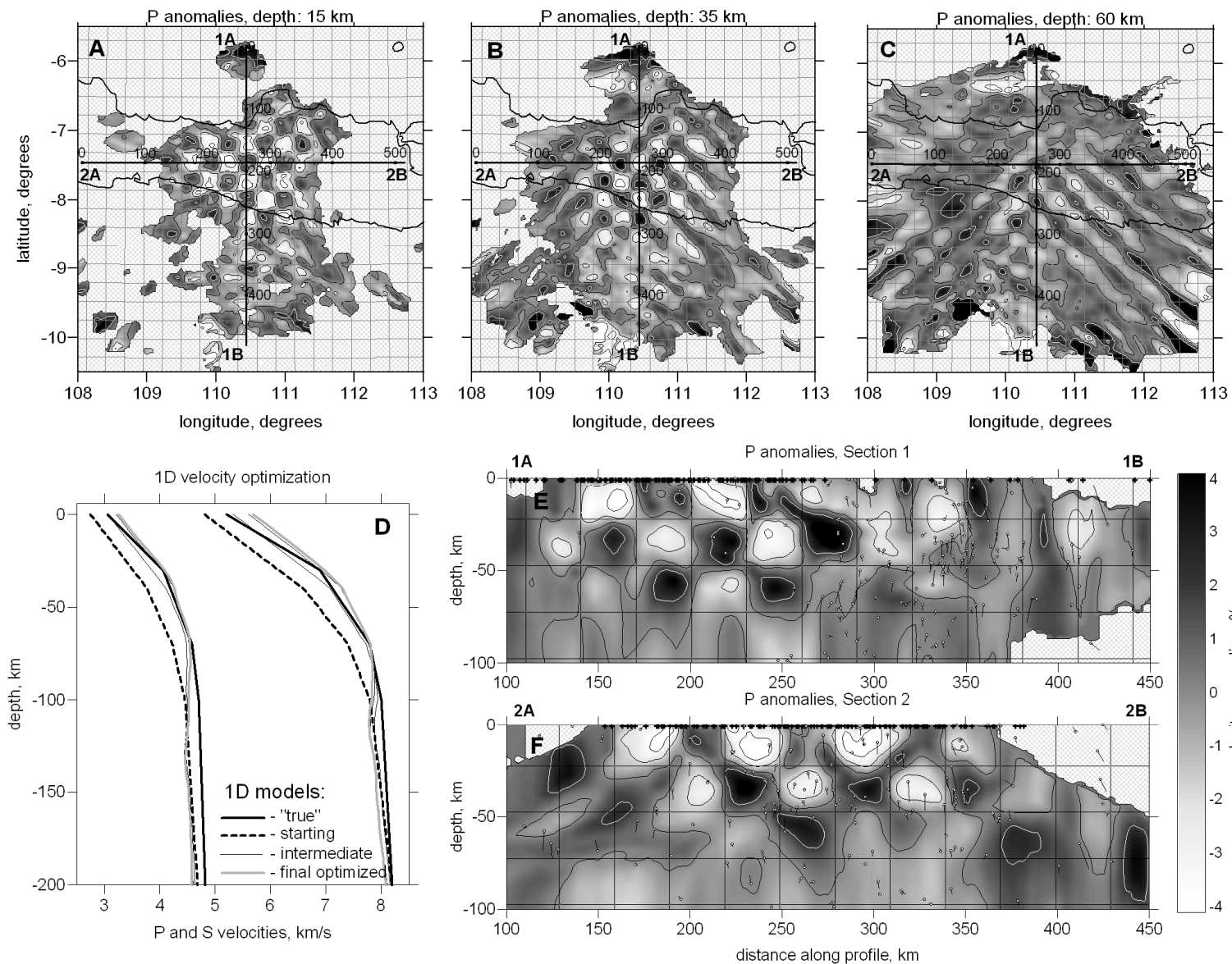
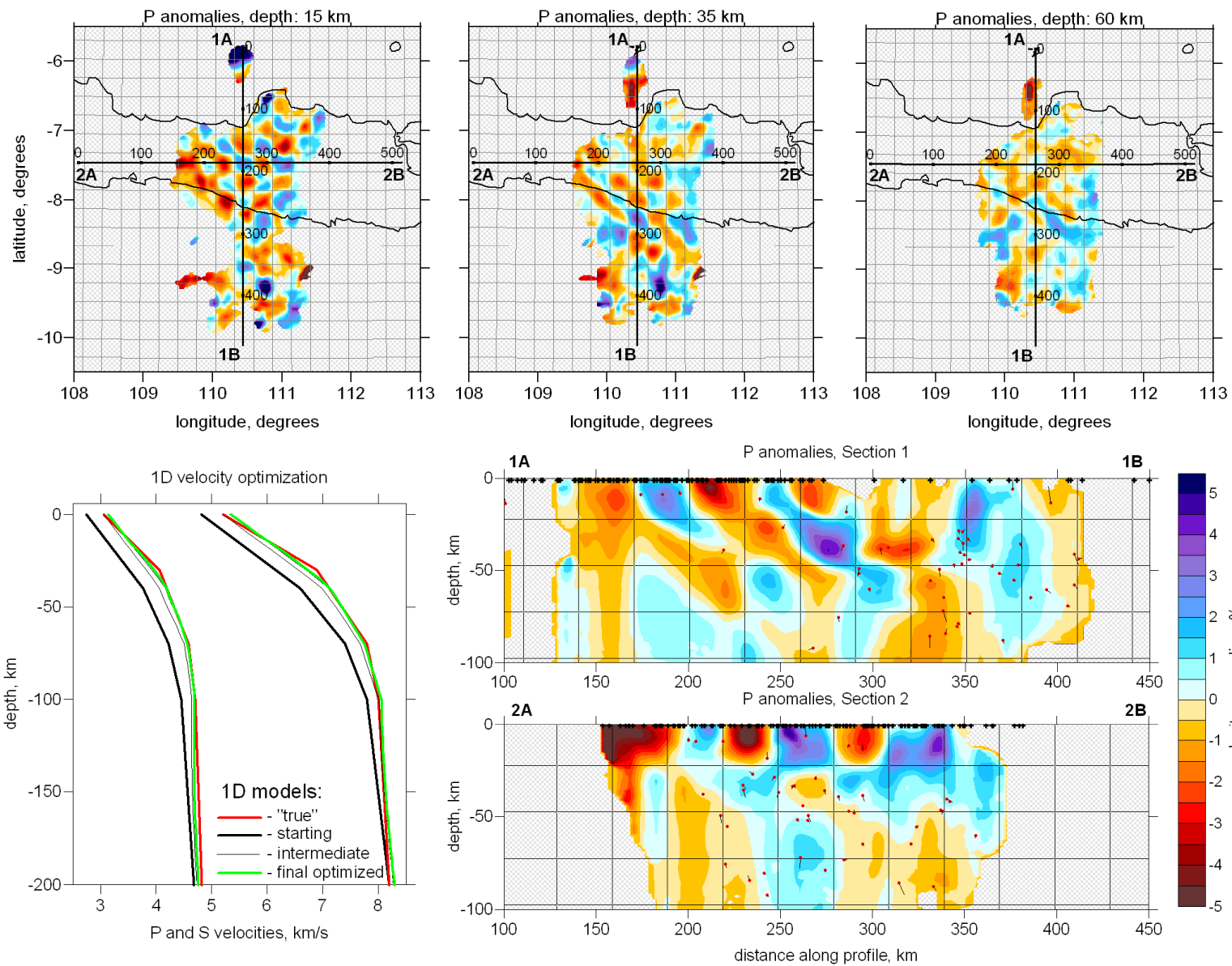
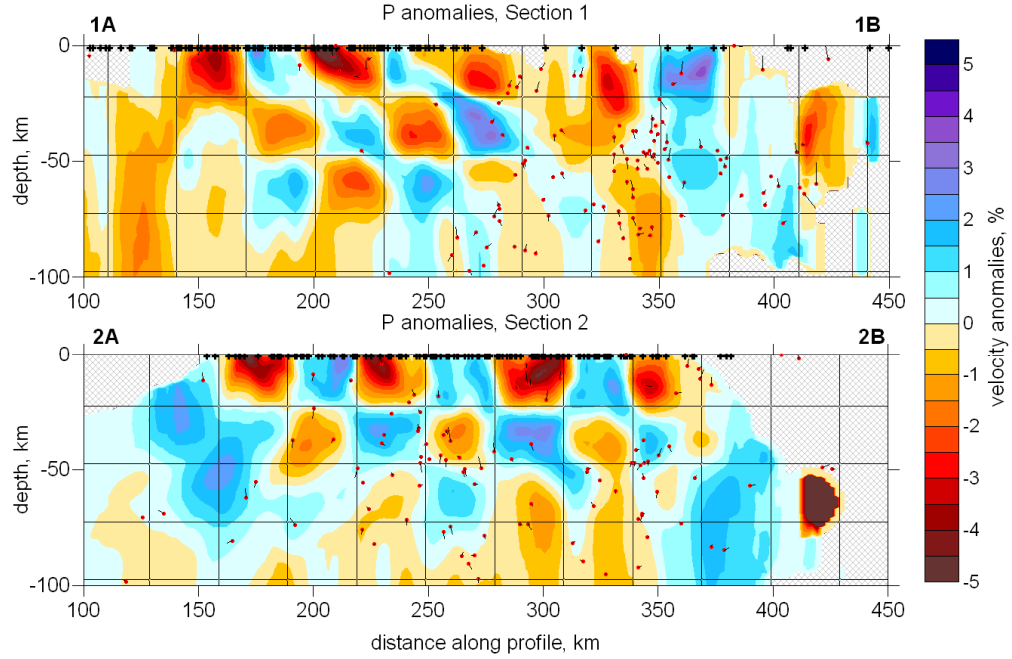
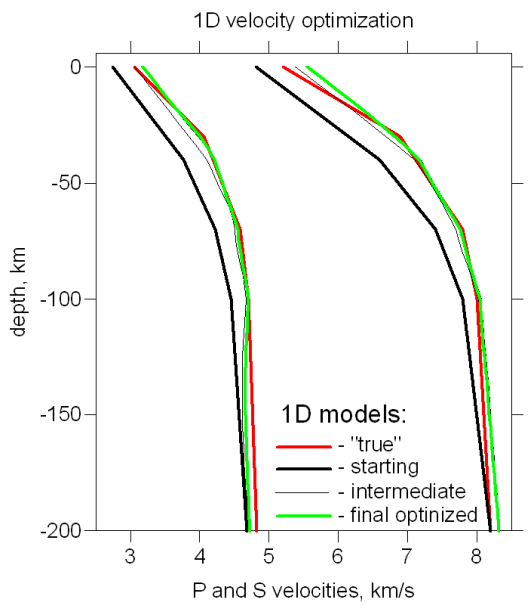
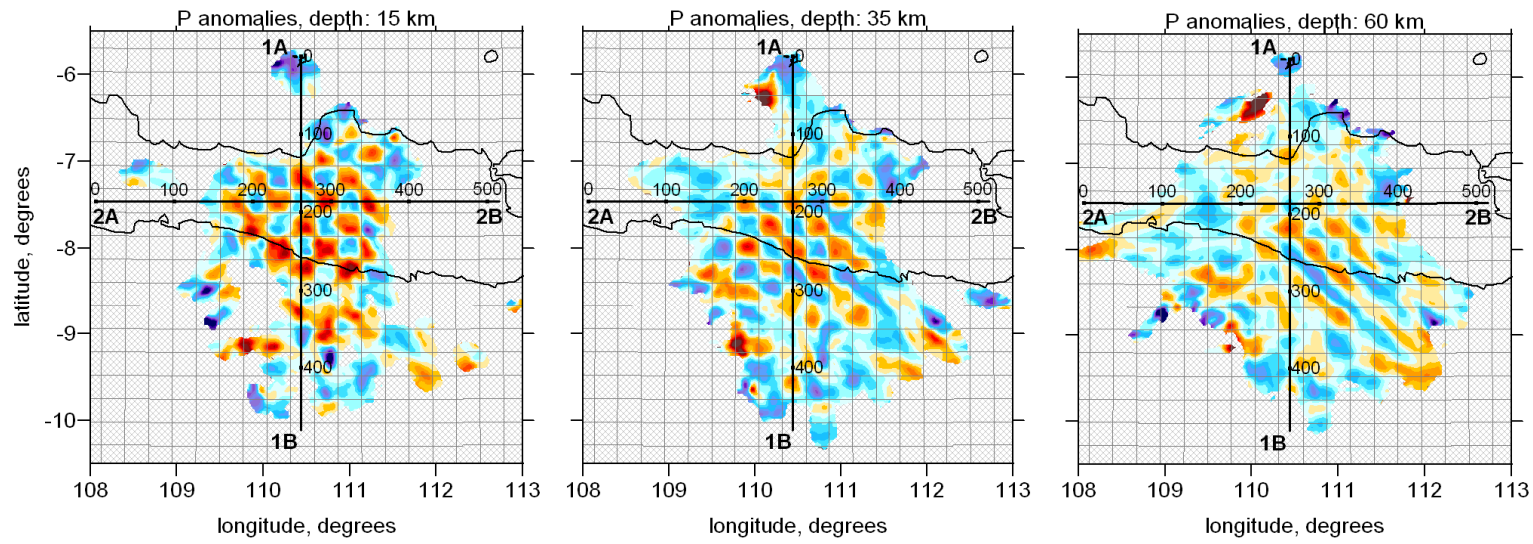


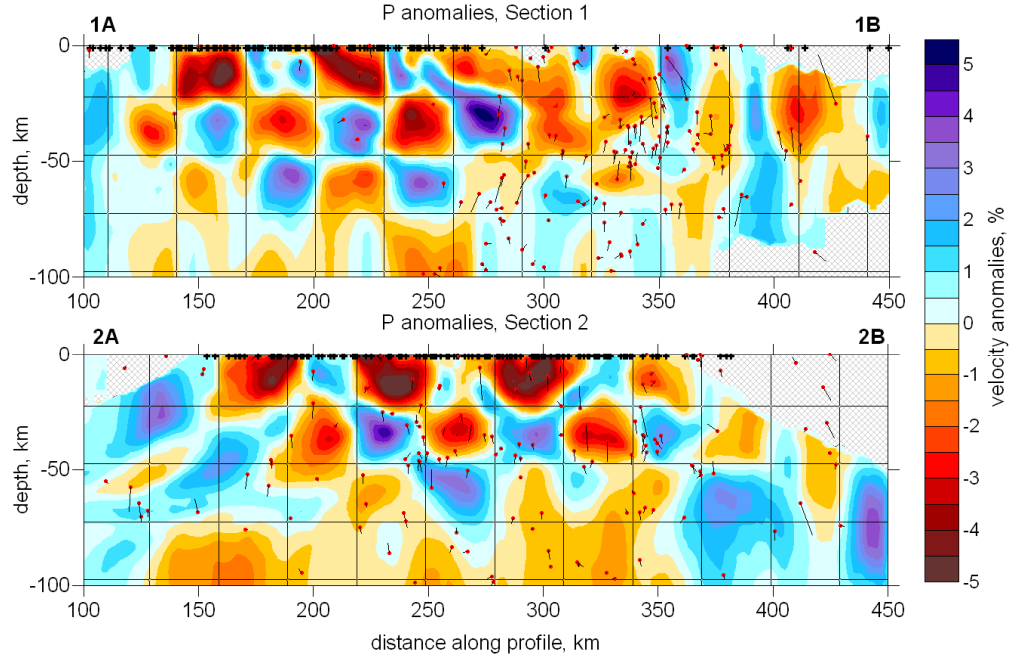
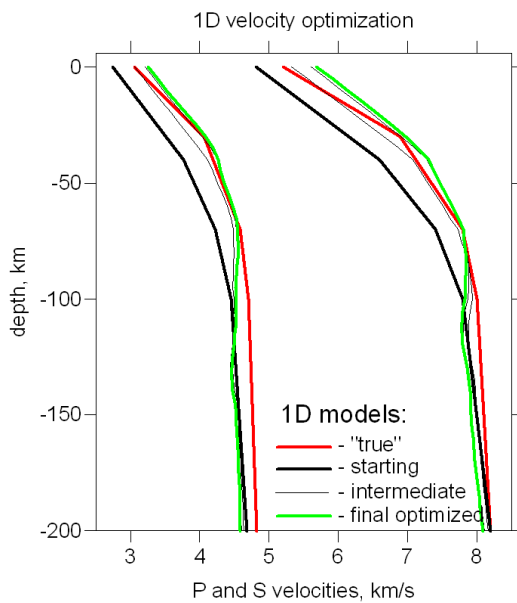
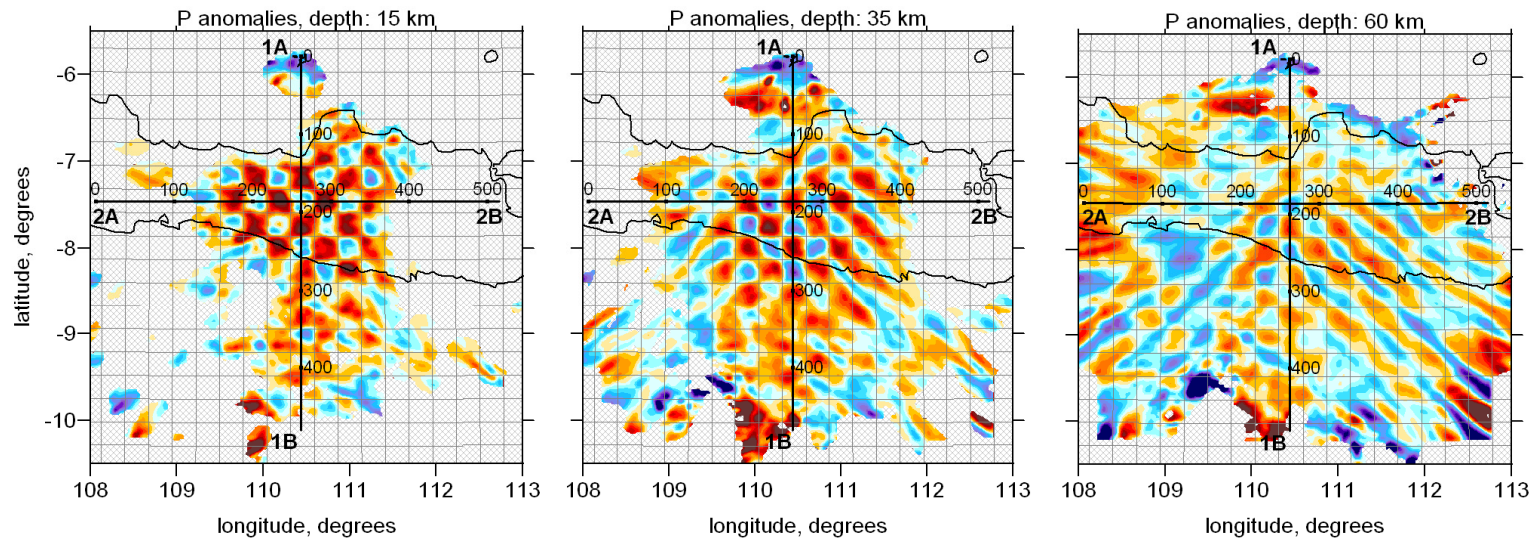
Figure 5. Inversion results using all sources within the area of  $5^\circ$  with respect to the center of the network. Meaning of plots and symbols are the same as in Figure 3. (Color version: Electronic Supplementary 3)



Electronic supplementary 1. Same as Figure 3, but in colors



Electronic supplementary 2. Same as Figure 4, but in colors



Electronic supplementary 3. Same as Figure 5, but in colors